Osteoarthritis and Cartilage 18 (2010) 1570–1576

Osteoarthritis and Cartilage

OARSI OSTEOARTHRITIS RESEARCH SOCIETY INTERNATIONAL

Simultaneous ultrasound measurement of articular cartilage and subchondral bone

A.S. Aula †*, J. Töyräs †‡, V. Tiitu §, J.S. Jurvelin †

† *Department of Physics and Mathematics, University of Eastern Finland, POB 1627, 70211, Kuopio, Finland*
‡ *Department of Clinical Neurophysiology, Kuopio University Hospital, POB 1777, 70211, Kuopio, Finland*
§ *Institute of Biomedicine, Anatomy, University of Eastern Finland, POB 1627, 70211, Kuopio, Finland*

ARTICLE INFO

Article history:
Received 30 March 2010
Accepted 24 September 2010

Keywords:
Ultrasound
Articular cartilage
Subchondral bone
Proximal tibia
Mechanical properties
pQCT

SUMMARY

Objective: In osteoarthritis (OA), subchondral sclerosis takes place during cartilage degeneration. High frequency ultrasound (12–55 MHz) has been shown to diagnose degenerated articular cartilage, while 0.1–1 MHz ultrasound has been applied for clinical characterization of bone and diagnostics of osteoporosis. The aim of the study is to investigate, for the first time, the feasibility of 5 MHz ultrasound for simultaneous analysis of articular cartilage and subchondral bone.

Methods: Osteochondral samples ($n = 10$) were prepared from fresh and visually normal bovine medial tibial plateaus. Acoustic properties of the cartilage and subchondral bone were measured with a scanning ultrasound system using the pulse-echo geometry and compared with biomechanical, histological and compositional reference data.

Results: The apparent integrated backscatter (AIB) from internal cartilage showed significant partial correlations with hydroxyproline (Hypro) ($r = 0.58$, $P = 0.000$), water content ($r = -0.52$, $P = 0.001$) and dynamic modulus ($r = 0.57$, $P = 0.000$) of the tissue. Weak but statistically significant correlation was found between the bone AIB and mineral density of the subchondral plate ($r = -0.34$, $P = 0.041$). Topographical variations in cartilage thickness could be detected using ultrasound. Composition, thickness and mechanical properties of the cartilage varied significantly across the tibial plateau. For the calculated ultrasound parameters, the variation was significant only between a few locations.

Conclusions: Pulse-echo ultrasound geometry at 5 MHz was feasible for simultaneous measurement of the acoustic properties of articular cartilage and subchondral bone. However, the relationships between the ultrasound parameters and properties of cartilage and bone were not as strong as reported earlier in studies focusing only either on bone or cartilage. Simultaneous measurement of both tissues compromises, due to natural curvature of articulating surfaces, the perpendicularity of the incidence of the ultrasound pulse. Obviously, this source of uncertainty should be minimized in order to enable effective clinical use of ultrasound in simultaneous measurement of articular cartilage and subchondral bone.

Introduction

Osteoarthritis (OA) is estimated to cause symptoms in 20–40% of elderly population[1]. Since the disease is, according to current knowledge, irreversible, early diagnosis would be imperative for prevention or slowing down further damage. Unfortunately, OA diagnosis is often delayed and current diagnostic techniques, *e.g.*, arthroscopy or radiographs, can typically detect OA when cartilage tissue is already severely damaged. Obviously, more sensitive quantitative techniques are needed to improve OA diagnostics and monitor the effects of OA treatments.

OA is characterized by disruption of the collagen network, depletion of the proteoglycans (PG), increase of water content and deterioration of mechanical properties of cartilage[2]. Previous studies suggest that the superficial cartilage contributes especially to the mechanical function of cartilage under dynamic mechanical loading[3,4]. When the superficial layer is damaged, mechanical properties of cartilage deteriorate and degenerative changes begin to accumulate. As the degradation of superficial cartilage, highly important to mechanical function of the tissue, is amongst the first signs of OA, its early detection would be of diagnostic importance.

Subchondral sclerosis and osteophyte formation are known to appear parallel to cartilage degeneration[2,5]. Radin and Rose[6]

* Address correspondence and reprint requests to: Antti S Aula, Department of Physics and Mathematics, University of Eastern Finland, P. O. Box 1627, FI-70211 Kuopio, Finland. Tel: 358-17-162342; Fax: 358-17-162585.
E-mail address: Antti.Aula@uef.fi (A.S. Aula).

1063-4584/$ – see front matter © 2010 Osteoarthritis Research Society International. Published by Elsevier Ltd. All rights reserved.
doi:10.1016/j.joca.2010.09.009

suggested that subchondral sclerosis, which causes thickening and stiffening of the subchondral plate, exposes cartilage to increased stresses, thus initiating the degeneration process. Further studies have shown the phenomenon to be more complex and to involve changes in bone density[7–9] and collagen content[10], which potentially lead to weakened subchondral trabecular bone[11]. Changes in the three-dimensional architecture of subchondral trabecular matrix are also involved in OA; bone volume fraction increases due to thickening of trabeculae, while number and separation of trabeculae decrease[12]. Moreover, trabecular matrix becomes more isotropic and plate-like in osteoarthritic joints[13].

In the proximal tibia the highest stresses during locomotion are measured in the medial condyle[14]. Due to variation in loading conditions, the mechanical properties of both bone and cartilage vary significantly across the proximal tibia. Cartilage is thicker in central areas, not covered by the meniscus, and gets thinner towards the edges of the joint[15]. Beneath the menisci, the density and mechanical strength of subchondral bone gradually decrease towards the margins of the condyle[14,15]. The meniscus is known to distribute the forces within the knee and hence prevent excessive loading of the cartilage[16]. Noble and Alexander suggested that meniscus, cartilage and subchondral bone have a trinitarian relationship where changes in any component cause adaptive changes in the other two tissues[15]. In that study, the density of the subchondral bone was reported to have an inverse relationship with the thickness of the meniscus and a direct relationship with the thickness of the cartilage. For these reasons, the medial condyle of proximal tibia is a good region to study the feasibility of ultrasound in a simultaneous analysis of cartilage and subchondral bone.

High frequency ultrasound (12–55 MHz) has been shown to detect spontaneous, enzymatically and mechanically generated changes in articular cartilage[17–19]. Typically, the analysis is based on measurement of ultrasound reflection from the surface of the cartilage but a few studies have shown that also backscattered signal recorded from the internal cartilage is related to the integrity of the tissue[20,21]. Unfortunately, the drawback of using high frequency ultrasound is high attenuation, which inevitably prevents analysis of the subchondral bone. A potential new method for arthroscopic ultrasound measurements of cartilage integrity was introduced recently[22,23]. The method applies a commercially available and clinically approved intra-vascular ultrasound (IVUS) catheter and could be, in principle, used for simultaneous measurement of cartilage and bone. A recent study reported qualitative and quantitative differences in the surface roughness and internal structure, measured with IVUS, between intact and repaired rabbit cartilage[24].

Pulse-echo ultrasound measurements have been successfully used for quantitative analysis of bone properties[25,26]. Reflection and backscatter provide information about the amount, composition, microstructure and mechanical properties of bone[27–30]. Frequencies 0.1–1 MHz have been suggested as the most useful for bone characterization[31], but higher frequencies (1–5 MHz) have also been successfully applied in several studies[26,28,29]. Low frequencies used for bone measurements, however, may lack the resolution necessary for the analysis of articular cartilage. In order to simultaneously analyze both tissues, an appropriate compromise has to be made when choosing the frequency.

The bovine knee joint is a widely used model in cartilage research. Several differences, as compared to human cartilage, are evident, *e.g.*, the size of the joint is larger, the thickness of the cartilage is smaller and the menisci cover relatively larger area in the bovine knee. However, the general tissue structure and shape are rather similar.

A natural circumstance for an *in vivo* high frequency ultrasound measurement of articular cartilage and subchondral bone is arthroscopy. Such an environment requires fast and simple measurements, so it is important to know whether optimal measurement conditions are needed for estimation of the integrity of cartilage and subchondral bone. Our hypothesis is that 5 MHz ultrasound could provide diagnostically valuable information on the quality of both cartilage and subchondral bone. To test this hypothesis, the present study investigates, for the first time, the feasibility of 5 MHz pulse-echo ultrasound measurements in simultaneous quantification of the properties of articular cartilage and subchondral bone.

Materials and methods

Visually normal bovine osteochondral samples ($n = 10$) were prepared from the knees of 10 animals within 6 h post mortem. Rectangular samples (width 30 mm, length 50 mm, height 20 mm) were cut with a band saw in medio-lateral direction across the medial tibial plateaus (Fig. 1). During the preparation, the samples were kept moist with phosphate buffered saline (PBS). The samples were stored in a freezer (−20°C) and thawed prior to the measurements. During the experiments and storing, the samples were immersed in PBS containing inhibitors of metalloproteinases, 5 mM ethylenediamine-tetraacetic acid, -disodium salt (EDTA, VWR International, Fontenay, France) and 5 mM benzamidine hydrochloride (Sigma–Aldrich Inc., St. Louis, MO, USA).

Acoustic properties of the cartilage and subchondral bone were measured with a scanning ultrasound system (UltraPac, Physical Acoustics Corporation, Princeton, NJ, USA) operating at 500 MHz sampling frequency. Pulse-echo parameters were measured with a 5 MHz ultrasound transducer (V307, GE Panametrics, Waltham, MA, USA). The −6 dB bandwidth and central frequency of the transducer were 3.2–6.7 MHz and 5.0 MHz, respectively. Ultrasound signals were recorded along a 30 mm long scan line using 0.15 mm lateral displacement steps between two recordings (Fig. 1). Before the ultrasound measurements, the ends of the scan line were manually set to the same horizontal plane using two orthogonal goniometers (Edmund Optics Ltd, York, UK). In addition, a rough time-of-flight scout scan was used to verify the optimal alignment of the samples before the actual ultrasound measurements. The signal gain was automatically optimized in every measurement point to avoid saturation of the signal and maximize the signal-to-noise ratio.

For the analyses, the sample area was divided into four anatomical locations. Location 1 was the most lateral and location 4 the most medial site of the medial tibial condyle (Fig. 1). The following ultrasound parameters were calculated: integrated reflection coefficient for saline-cartilage interface (IRC_{cart}) and cartilage-bone interface (IRC_{bone}), apparent integrated backscatter

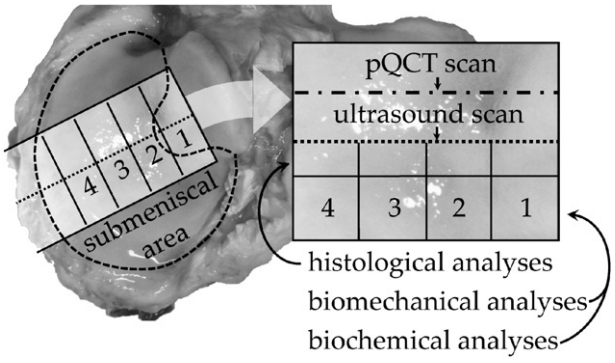

Fig. 1. The anatomical locations of the test sites (numbers), reference and ultrasound (dot line) measurements in the medial tibial plateau of a bovine knee. The edge of the meniscus is illustrated with a dash line.

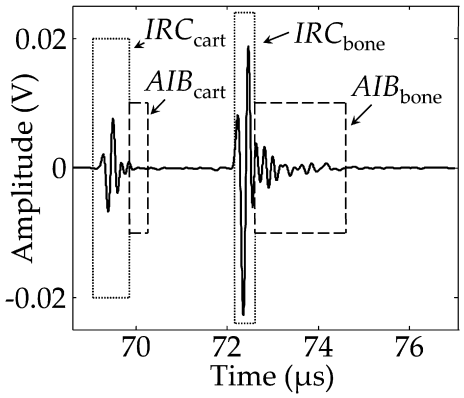

Fig. 2. Typical ultrasound pulse-echo signal from an osteochondral sample. Signals from the cartilage and bone can be detected and separated for cartilage thickness down to 0.2 mm. The present IRC time windows were chosen to include the whole reflection waveform from all samples: 0.8 μs for IRC_{cart} and 0.4 μs for IRC_{bone}. Time window for AIB_{cart} was 0.4 μs, which allowed use of a fixed time window also for the thinnest cartilage samples. Time window for AIB_{bone} was 2 μs.

from internal structures of cartilage (AIB_{cart}) and subchondral bone (AIB_{bone}) and ultrasound roughness index (URI) for cartilage surface (Fig. 2)[33,34]. Mathematical definitions of the parameters are presented in Table I. The IRC time windows were chosen wide enough to include the whole reflection waveform from all samples: 0.8 μs for IRC_{cart} and 0.4 μs for IRC_{bone}. Time window for AIB_{cart} was 0.4 μs, which allowed determination of cartilage AIB at all measurement sites. The time window for AIB_{bone} was fixed to 2 μs for all samples. Fixed time window may cover longer region in the samples with larger bone volume fraction, because the speed of sound is larger in bone tissue than in bone marrow.

The thickness of the cartilage was estimated using the time-of-flight data from the saline-cartilage and cartilage-bone boundaries. The speed of sound for cartilage was assumed to be 1602 m/s in tibial cartilage[35]. This thickness information was only used for setting the parameters of the mechanical testing protocol. If the transducer is not perpendicular to the cartilage or bone surfaces, part of the ultrasound reflection misses the transducer, which causes underestimation of the reflection. To consider this, the angles between the transducer and tissue boundaries were measured and used as controlling variables in the partial correlation analyses. The angles of incidence between the ultrasound pulse and saline-cartilage or cartilage-bone interfaces were calculated using the time-of-flight information and a 20 measurements

Table I
Mathematical definitions of the ultrasound parameters

Parameter	Equation
IRC[33,44]	$\frac{1}{\Delta f}\int_{\Delta f} 10\cdot\log_{10}\left\langle\frac{\lvert A_R(f,z)\rvert^2}{\lvert A_0(f,z)\rvert^2}\right\rangle \mathrm{d}f$
AIB[33,44]	$\frac{1}{\Delta f}\int_{\Delta f} 10\cdot\log_{10}\left\langle\frac{\lvert A_{BS}(f,z)\rvert^2}{\lvert A_0(f,z)\rvert^2}\right\rangle \mathrm{d}f$
URI[34]	$\sqrt{\frac{1}{m}\sum_{i=1}^{m}(d_i-\langle d\rangle)^2}$

$A(f,z)$ = Amplitude spectrum of a pulse recorded at distance z from the transducer
f = Frequency
Δf = Frequency range corresponding to −6 dB bandwidth
m = Number of measurement points
d_i = Distance between the transducer and cartilage surface
$\langle d\rangle$ = Average distance between the transducer and cartilage surface
$\langle\rangle$ = Spatial average
Indices *R*, *BS* and zero refer to reflected signal from the interfaces of saline-cartilage and cartilage-bone, backscattered signal from internal structures of cartilage and bone, and signal received from a perfect reflector, respectively.

(3 mm) wide moving window at each measurement point. The local inclination was estimated from the slope of a linear fit in the moving window. After the ultrasound measurements, the samples were cut into two halves along the ultrasound scan line. One half was scanned with a pQCT device and used in another study[36], while the other half was prepared for further biochemical, histological and biomechanical analyses (Fig. 1).

Dynamic modulus (E_{dyn}) and Young's modulus (E_{Young}) of cartilage were determined with a custom made material testing device[37] and a cylindrical plane-ended (dia = 1.13 mm) indenter. After applying 12.5 kPa pre-strain, four stress-relaxation steps (strain 5%) were performed to equilibrium (relaxation time 900 s). The accurate thickness of the cartilage at the indentation site was measured with the needle probe technique[38] and the information was used for calculation of the mechanical moduli. Dynamic modulus was calculated from the third stress-relaxation step and Young's modulus as the slope of equilibrium stress–strain curve fit to the last three stress-relaxation steps. The modulus values were calculated using an elastic isotropic model, according to Hayes *et al.*[39]. For calculation of the dynamic modulus of cartilage, the Poisson ratio was set to 0.5 (*i.e.*, dynamically incompressible), while at equilibrium the Poisson ratio was set to 0.1[40].

Safranin-O stained microscopic sections were cut for qualitative histological imaging of the spatial PG distribution (Fig. 3). The samples were fixed in 4% formaldehyde in 0.07 M phosphate buffer (pH 7.0), decalcified with 10% EDTA in phosphate buffer (pH 7.4), and processed through a series of ethanol solutions (50%, 80%, 94%, 94%, 94% and twice absolute ethanol), twice in xylene, and twice in melted Paraplast Plus wax (Sherwood Medical Co, St. Louis, MO, USA). After embedding, microscopic sections (3 μm thick) were prepared and stained with 0.5% (w/v) safranin-O[41] in 0.1 M sodium acetate buffer (pH 4.6).

Biochemical analyses were used to determine the water content and the amounts of uronic acid (UA) and hydroxyproline (Hypro) in the tissue. The cartilage was detached from the bone with a razor blade. After measuring the wet weights of the samples, they were freeze-dried, and the dry weights of the samples were determined. The dried samples were incubated with a 1 mg/mL concentration of papain (Sigma–Aldrich Inc.) in 150 mM sodium acetate including 50 mM Cys–HCl (Sigma–Aldrich Inc.) and 5 mM EDTA (Merck, Darmstadt, Germany), pH 6.5, for 3 h at 60°C. The samples were boiled for 10 min to inactivate the enzyme. The UA contents of the digests were quantitated from the ethanol-precipitated samples[42]. The amounts of UA were normalized to the wet weights of the samples to compensate for the variation in the sample sizes. To estimate the collagen content of the samples, spectrophotometric assay for Hypro was performed after hydrolysis of the freeze-dried and papain digested tissue[43]. Hypro contents were normalized against the wet weights of the samples.

The bone mineral densities of the subchondral plate (BMD_{plate}) and subchondral trabecular bone (BMD_{trab}) were measured with a pQCT device (XCT 2000, Stratec Medizintechnik GmbH, Pforzheim, Germany). The thickness of the pQCT slice was 2.3 mm and the in-plane pixel size was 0.2 × 0.2 mm^2.

The data was analyzed with Matlab 7.4 (MathWorks Inc., Natick, MA, USA). R Statistical Software version 2.11.1 (R Foundation for Statistical Computing, Vienna, Austria) was used for statistical tests. The Shapiro–Wilk test was used to test the normality of the data and the Friedman's *post-hoc* test to determine the statistical significance of topographical variation between the locations. The Spearman's rho and partial correlation analyses were used for testing the associations between the parameters. In partial correlation analysis the controlling parameter for the cartilage parameters was the angle of incidence of ultrasound at the cartilage surface. For bone parameters the controlling parameters were the

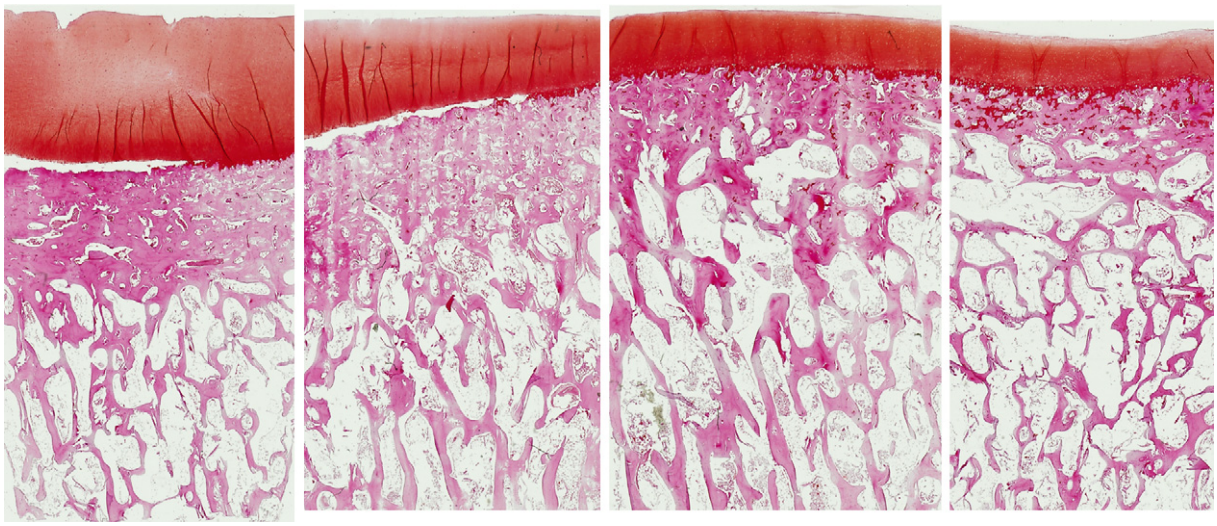

Fig. 3. Safranin-O stained histological sections across the medial tibial plateau demonstrate the spatial variation in structure and composition of cartilage and subchondral bone. Thicknesses of cartilage and subchondral plate can be seen to decrease towards the margin of the joint. Also the curvature of the medial plateau is well demonstrated in the figure.

angles of incidence of ultrasound pulse at the cartilage surface and bone-cartilage interface and the thickness of the cartilage.

Results

Ultrasound backscatter (AIB) from the internal cartilage correlated significantly with Hypro ($r = 0.58$, $P = 0.000$) and water contents ($r = -0.52$, $P = 0.001$) and dynamic modulus ($r = 0.57$, $P = 0.000$) of the tissue. There was also a significant negative correlation ($r = -0.55$, $P = 0.000$) between the ultrasound backscatter and the thickness of the cartilage. The water content, thickness and mechanical moduli of cartilage were also found to correlate with the ultrasound roughness index of the tissue surface (Table II). Weak but statistically significant correlation was found ($r = -0.34$, $P = 0.041$) between the bone AIB and BMD of the subchondral plate.

Thickness, composition and mechanical properties of cartilage varied significantly across the tibial plateau (Tables III and IV). Site-to-site variations in the ultrasound roughness index and reflection from the cartilage-bone boundary were statistically significant only between a few locations. The topographical variation was more pronounced for composition, thickness and mechanical properties of cartilage and mineralization of bone.

Correlations between the cartilage thickness, composition and mechanical properties varied from moderate to good. The properties of cartilage, however, were not found to correlate with the mineralization of bone (Table V). The correlation coefficient between the two values of cartilage thickness, measured with the needle probe and ultrasound, was $r = 0.89$ ($P = 0.000$).

Discussion

The pulse-echo ultrasound geometry at 5 MHz was feasible for simultaneous measurement of the acoustic properties of articular cartilage and subchondral bone. Backscattered signal from the internal cartilage correlated with the water content, mechanical properties, thickness and especially with the collagen content of the cartilage. This finding is in line with earlier findings using high frequency ultrasound[44]. Furthermore, ultrasound backscatter from subchondral bone correlated with the BMD, which is consistent with findings using lower ultrasound frequencies[28].

Thickness, composition and mechanical properties of cartilage varied significantly across the tibial plateau. Ultrasound backscatter and ultrasound roughness index were able to detect part of this variation in cartilage. BMD of the subchondral plate and trabecular region, bone IRC and bone AIB also varied significantly across the sample. Variation in bone ultrasound parameters, however, is probably partly due to variation in cartilage thickness. Thick cartilage attenuates ultrasound effectively, leading to underestimation of these ultrasound parameters. The same phenomenon improves correlations between the bone ultrasound and cartilage reference parameters. However, the authors decided not to numerically adjust the measured ultrasound signals with cartilage thickness or angles of incidence of the ultrasound pulse and tissue layers,

Table II
AIB_{cart} and URI from cartilage correlated significantly with the composition, mechanical properties and thickness of cartilage, while AIB_{bone} correlated with bone mineral density of subchondral plate (BMD_{plate}). In partial correlation analysis the controlling parameter for the cartilage parameters was the angle of incidence of the ultrasound at the cartilage surface. For bone parameters the controlling parameters were the angles of incidence of the ultrasound pulse at the cartilage surface and bone-cartilage interface and thickness of the cartilage

	UA	Hypro	Water	E_{Dyn}	E_{Young}	Thickness	BMD_{plate}	BMD_{trab}
AIB_{cart}	0.01	**0.58****	**−0.52****	**0.57****	0.16	**−0.55****	−0.11	−0.20
IRC_{cart}	−0.13	−0.16	0.16	−0.05	−0.06	0.10	0.14	**−0.36***
URI	−0.28	−0.29	**0.47****	**−0.49****	**−0.41****	**0.56****	0.08	0.09
AIB_{bone}	0.24	0.00	−0.01	−0.06	0.04	–	**−0.34***	−0.05
IRC_{bone}	0.02	−0.02	0.18	−0.29	−0.21	–	0.09	−0.05

*$P < 0.05$
**$P < 0.01$

Table III
The Friedman's *post-hoc* test revealed that the topographical variation between the measurement locations was statistically significant for all parameters but the ultrasound reflection from the surface of the cartilage. The variation was more pronounced for composition, thickness and mechanical properties of cartilage and mineralization of bone, while the ultrasound measurements were able to detect only part of this variation in cartilage. Only *P*-values below 0.05 are presented in the table

Locations	All	1–2	1–3	1–4	2–3	2–4	3–4
Cartilage parameters							
AIB_{cart}	**0.000**	–	–	**0.017**	–	**0.000**	**0.029**
IRC_{cart}	–	–	–	–	–	–	–
URI	**0.046**	–	**0.046**	–	–	–	–
UA	**0.001**	–	**0.001**	–	**0.046**	–	–
Hypro	**0.003**	–	**0.010**	**0.003**	**0.029**	**0.010**	–
Water	**0.000**	–	**0.003**	**0.000**	–	–	–
Thickness	**0.000**	–	**0.002**	**0.000**	–	**0.005**	–
E_{Dyn}	**0.000**	–	**0.001**	**0.000**	–	**0.006**	–
E_{young}	**0.000**	–	**0.000**	**0.005**	**0.046**	–	–
Bone parameters							
AIB_{bone}	**0.000**	–	**0.002**	**0.000**	–	–	–
IRC_{bone}	**0.000**	–	**0.000**	**0.005**	**0.046**	–	–
BMD_{plate}	**0.029**	–	–	–	–	**0.028**	**0.046**
BMD_{trab}	**0.006**	**0.028**	**0.047**	–	–	**0.005**	**0.010**

because assumptions needed for such correction factors could have compromised the reliability of the data. Instead, the partial correlation analysis was considered to provide a more appropriate way to deal with these sources of uncertainty.

Based on the present results, ultrasound backscatter (AIB) and roughness index (URI) seemed to be rather insensitive to the angle of incidence of the ultrasound pulse. Ultrasound reflection (IRC), however, is known to be highly sensitive to angle of incidence[45,46], which explains the lack of significant correlations between the reflection parameters and the reference parameters. According to Wilhjelm *et al.*, inclination of three degrees is enough to reduce the signal energy by −6 dB[46]. Kaleva *et al.* suggested that the scattering becomes the dominant source of signal instead of specular reflection for inclinations over two degrees. However, they reported that degraded cartilage could be distinguished from intact at articular surface inclinations up to five degrees[45]. In the present study, average angles of incidence (±standard deviation (SD)) of the ultrasound pulse at the cartilage and bone surfaces were 4.6 ± 3.0 and 5.9 ± 3.2 degrees, respectively. Most of previous *in vitro* studies have carefully positioned cartilage surface perpendicular to the ultrasound beam. This, however, was impossible in the present study with a larger sample size, scan length and natural curvature of the tibial plateau. The same applies for bone ultrasound measurements; *in vitro* studies often apply samples with perfectly flat surfaces and no cortical layer. However, the cortical layer has been shown to reduce the accuracy of ultrasound measurements[47–49]. If the angle between the transducer and the bone surface deviates enough from the perpendicular alignment, reflected ultrasound beam misses the transducer completely and the recorded signal consists solely of scattered signal. Moreover, curved bone surfaces distort the ultrasound signal also in the through-transmission geometry. This effectively compromises the measurement and should be carefully considered when designing ultrasound measurements.

Table IV
The mean values (±SD) of the measured ultrasound parameters, thickness, composition and mechanical properties of cartilage and BMDs of subchondral bone. Location describes the site of the measurement, 1 being the most lateral and 4 the most medial site of the medial tibial condyle (Fig. 1). See Table III for the statistical significance of variation between the locations

Location	1	2	3	4
Cartilage parameters				
AIB_{cart} (dB)	-72 ± 3	-73 ± 4	-70 ± 6	-65 ± 5
IRC_{cart} (dB)	-42 ± 7	-41 ± 5	-41 ± 8	-42 ± 5
URI (μm)	70 ± 46	33 ± 19	30 ± 20	35 ± 25
UA (μg/mg)	4.5 ± 0.7	5.0 ± 0.9	6.5 ± 0.9	5.4 ± 1.4
Hypro (μg/mg)	6.6 ± 1.6	7.8 ± 1.1	10.2 ± 0.9	12.1 ± 2.8
Water (%)	89 ± 1	87 ± 2	84 ± 1	84 ± 1
Thickness (mm)	3.1 ± 0.4	2.2 ± 0.4	1.6 ± 0.4	1.0 ± 0.2
E_{Dyn} (MPa)	0.4 ± 0.2	1.2 ± 0.9	4.1 ± 2.4	7.7 ± 2.8
E_{Young} (MPa)	0.2 ± 0.0	0.3 ± 0.2	0.9 ± 0.2	0.7 ± 0.3
Bone parameters				
AIB_{bone} (dB)	-40 ± 4	-36 ± 3	-34 ± 2	-34 ± 2
IRC_{bone} (dB)	-32 ± 7	-25 ± 4	-22 ± 4	-23 ± 4
BMD_{plate} (mg/cm^3)	870 ± 53	882 ± 49	883 ± 58	820 ± 87
BMD_{trab} (mg/cm^3)	483 ± 42	534 ± 59	536 ± 47	457 ± 36

Table V
Spearman's correlation coefficients between the cartilage thickness, composition and mechanical properties were significant. The properties of cartilage, however, were not found to correlate with the mineralization of subchondral bone

	Hypro	Water	E_{Dyn}	E_{Young}	Th_{Cart}	BMD_{plate}	BMD_{trab}
UA	**0.42****	**−0.50****	**0.44****	**0.69****	−0.31	−0.24	0.28
Hypro	–	**−0.75****	**0.76****	**0.55****	**−0.79****	−0.18	−0.11
Water		–	**−0.89****	**−0.79****	**0.81****	0.12	−0.02
E_{Dyn}			–	**0.82****	**−0.95****	−0.24	−0.13
E_{Young}				–	**−0.68****	−0.11	0.18

$^{**}P < 0.01$.
$^{*}P < 0.05$.

The use of one optimized gain for each measurement is a simple and fast procedure, but also has certain drawbacks. The gain was optimized to maximize the signal-to-noise ratio of both the saline-cartilage and cartilage-bone reflections, *i.e.*, the gain may not have been optimal for the backscatter signal which is typically of a smaller magnitude. To simulate a straightforward clinical measurement, the gain was not optimized for each signal region. In clinical practice, diagnostic techniques should be fast, simple and easy to use.

Even though Kaleva *et al.* suggested that 5 MHz ultrasound is not sufficient for accurate measurement of the roughness of articular surface[32], in the present study the cartilage surface roughness, measured with ultrasound, was related to water content, mechanical properties and thickness of the tissue. This is in line with an earlier study using high frequency (20 MHz) ultrasound, in which a significant correlation between the URI and mechanical properties of cartilage was observed[18]. The URI values measured in this study are larger than the values reported earlier[32]. This discrepancy may be caused by the natural curvature of the samples, as the inclination of the cartilage surface has been reported to cause overestimation of the URI[45]. URI was the largest in the location 1 and significantly ($P = 0.046$) larger than that in the location 3. Even though the structure and composition of the locations varied significantly ($P < 0.01$), URI was not able to detect the variation between the locations 2, 3 and 4. This is possibly due to relatively low central frequency of the applied ultrasound transducer. The correlation coefficient between the values of cartilage thickness measured with the needle probe and ultrasound techniques was $r = 0.89$ ($P = 0.000$), suggesting good precision for cartilage thickness measurements using ultrasound. Feasibility of ultrasonic thickness measurements was expected, since the applied 5 MHz ultrasound transducer (half maximum full width of the pulse was 0.25 μs) is theoretically able to estimate cartilage thickness down to 0.2 mm[50].

The present results provide steps to which direction quantitative ultrasound techniques need to be developed. Elimination of the effects of overlying tissue layers and variation in the angles of incidence of the ultrasound pulse at reflecting surfaces are essential

for reliable quantification of the reflection and backscatter parameters. Therefore, further studies and innovative approaches are needed for optimization of the measurement protocol and minimization of the effect of overlying tissue layers. For example, application of a rotating ultrasound catheter[22,23] could diminish some of the error sources due to the curvature of the structures. It is one potential way to further develop simultaneous ultrasound measurement of cartilage and subchondral bone. However, the ultrasound frequency of the catheter used by Virén *et al.* is too high for ultrasound measurement of bone through a layer of cartilage. Fortunately, ultrasound catheters are commercially available at, for example, 9 MHz frequency (Boston Scientific Corporation, San Jose, CA, USA), which might be a more feasible frequency for simultaneous measurement of articular cartilage and subchondral bone *in vivo*.

To conclude, simultaneous measurement of articular cartilage and subchondral bone was conducted with 5 MHz pulse-echo ultrasound. Even though the ultrasound parameters were found to depend on the structure and composition of the cartilage, and mineral density of the bone, further studies are needed for optimization of the ultrasound frequency and measurement geometry.

Author contributions

All authors have substantially contributed to the conception and design of the study, acquisition of data, or analysis and interpretation of data. All authors have participated in the writing process and approved the final version of the manuscript. Antti Aula (antti.aula@uef.fi) takes responsibility for the integrity of the work.

Role of the funding sources

Sources of funding are Finnish Cultural Foundation, Finnish Foundation for Technology Promotion, Kuopio University Hospital, Finnish Ministry of Education and National Graduate School of Musculoskeletal Disorders and Biomaterials. The funding sources had no role in the study design, collection, analysis or interpretation of data; in the writing of the manuscript or in the decision to submit the manuscript for publication.

Conflict of interest

The authors have no conflicts of interest.

Acknowledgements

Financial support from Finnish Cultural Foundation, Finnish Foundation for Technology Promotion, Kuopio University Hospital, Finnish Ministry of Education and National Graduate School of Musculoskeletal Disorders and Biomaterials is acknowledged.

Supplementary data

Supplementary data associated with this article can be found in the online version, at doi:10.1016/j.joca.2010.09.009.

References

1. Felson DT. Epidemiology of hip and knee osteoarthritis. Epidemiol Rev 1988;10:1–28.
2. Buckwalter JA, Mankin HJ. Articular cartilage: degeneration and osteoarthritis, repair, regeneration, and transplantation. Instr Course Lect 1998;47:487–504.
3. Korhonen RK, Wong M, Arokoski J, Lindgren R, Helminen HJ, Hunziker EB, *et al*. Importance of the superficial tissue layer for the indentation stiffness of articular cartilage. Med Eng Phys 2002;24(2):99–108.
4. Glaser C, Putz R. Functional anatomy of articular cartilage under compressive loading. Quantitative aspects of global, local and zonal reactions of the collagenous network with respect to the surface integrity. Osteoarthritis Cartilage 2002;10(2):83–99.
5. Anderson-MacKenzie JM, Quasnichka HL, Starr RL, Lewis EJ, Billingham ME, Bailey AJ. Fundamental subchondral bone changes in spontaneous knee osteoarthritis. Int J Biochem Cell Biol 2005;37(1):224–36.
6. Radin EL, Rose RM. Role of subchondral bone in the initiation and progression of cartilage damage. Clin Orthop Relat Res 1986;213:34–40.
7. Wada M, Maezawa Y, Baba H, Shimada S, Sasaki S, Nose Y. Relationships among bone mineral densities, static alignment and dynamic load in patients with medial compartment knee osteoarthritis. Rheumatology (Oxford) 2001;40(5):499–505.
8. Bennell KL, Creaby MW, Wrigley TV, Hunter DJ. Tibial subchondral trabecular volumetric bone density in medial knee joint osteoarthritis using peripheral quantitative computed tomography technology. Arthritis Rheum 2008;58(9):2776–85.
9. Johnston JD, Masri BA, Wilson DR. Computed tomography topographic mapping of subchondral density (CT-TOMASD) in osteoarthritic and normal knees: methodological development and preliminary findings. Osteoarthritis Cartilage 2009;17(10):1319–26.
10. Mansell JP, Bailey AJ. Abnormal cancellous bone collagen metabolism in osteoarthritis. J Clin Invest 1998;101(8):1596–603.
11. Li B, Aspden RM. Composition and mechanical properties of cancellous bone from the femoral head of patients with osteoporosis or osteoarthritis. J Bone Miner Res 1997;12(4):641–51.
12. Bobinac D, Spanjol J, Zoricic S, Maric I. Changes in articular cartilage and subchondral bone histomorphometry in osteoarthritic knee joints in humans. Bone 2003;32(3):284–90.
13. Ding M, Odgaard A, Hvid I. Changes in the three-dimensional microstructure of human tibial cancellous bone in early osteoarthritis. J Bone Joint Surg Br 2003;85(6):906–12.
14. Hvid I, Hansen SL. Trabecular bone strength patterns at the proximal tibial epiphysis. J Orthop Res 1985;3(4):464–72.
15. Noble J, Alexander K. Studies of tibial subchondral bone density and its significance. J Bone Joint Surg Am 1985;67(2):295–302.
16. Radin EL, de Lamotte F, Maquet P. Role of the menisci in the distribution of stress in the knee. Clin Orthop Relat Res 1984;185:290–4.
17. Disler DG, Raymond E, May DA, Wayne JS, McCauley TR. Articular cartilage defects: in vitro evaluation of accuracy and interobserver reliability for detection and grading with US. Radiology 2000;215(3):846–51.
18. Saarakkala S, Laasanen MS, Jurvelin JS, Töyräs J. Quantitative ultrasound imaging detects degenerative changes in articular cartilage surface and subchondral bone. Phys Med Biol 2006;51(20):5333–46.
19. Saïed A, Cherin E, Gaucher H, Laugier P, Gillet P, Floquet J, *et al*. Assessment of articular cartilage and subchondral bone: subtle and progressive changes in experimental osteoarthritis using 50 MHz echography in vitro. J Bone Miner Res 1997;12(9):1378–86.
20. Wang SZ, Huang YP, Saarakkala S, Zheng YP. Quantitative assessment of articular cartilage with morphologic, acoustic and mechanical properties obtained using high-

frequency ultrasound. Ultrasound Med Biol 2010;36 (3):512–27.
21. Pellaumail B, Watrin A, Loeuille D, Netter P, Berger G, Laugier P, *et al*. Effect of articular cartilage proteoglycan depletion on high frequency ultrasound backscatter. Osteoarthritis Cartilage 2002;10(7):535–41.
22. Huang YP, Zheng YP. Intravascular ultrasound (IVUS): a potential arthroscopic tool for quantitative assessment of articular cartilage. Open Biomed Eng J 2009;3:13–20.
23. Virén T, Saarakkala S, Kaleva E, Nieminen HJ, Jurvelin JS, Töyräs J. Minimally invasive ultrasound method for intra-articular diagnostics of cartilage degeneration. Ultrasound Med Biol 2009;35(9):1546–54.
24. Virén T, Saarakkala S, Pulkkinen H, Tiitu V, Valonen P, Kiviranta I, *et al*. Quantitative evaluation of spontaneously and surgically repaired rabbit articular cartilage using a minimally invasive ultrasound method (abstract). Trans Orthop Res Soc 2010;35:996.
25. Hoffmeister BK, Johnson DP, Janeski JA, Keedy DA, Steinert BW, Viano AM, *et al*. Ultrasonic characterization of human cancellous bone in vitro using three different apparent backscatter parameters in the frequency range 0.6–15.0 MHz. IEEE Trans Ultrason Ferroelectr Freq Control 2008;55(7):1442–52.
26. Karjalainen JP, Töyräs J, Riekkinen O, Hakulinen M, Jurvelin JS. Ultrasound backscatter imaging provides frequency-dependent information on structure, composition and mechanical properties of human trabecular bone. Ultrasound Med Biol 2009;35(8):1376–84.
27. Chaffaï S, Peyrin F, Nuzzo S, Porcher R, Berger G, Laugier P. Ultrasonic characterization of human cancellous bone using transmission and backscatter measurements: relationships to density and microstructure. Bone 2002;30(1):229–37.
28. Hakulinen MA, Day JS, Töyräs J, Timonen M, Kröger H, Weinans H, *et al*. Prediction of density and mechanical properties of human trabecular bone in vitro by using ultrasound transmission and backscattering measurements at 0.2–6.7 MHz frequency range. Phys Med Biol 2005;50(8):1629–42.
29. Hoffmeister BK, Whitten SA, Kaste SC, Rho JY. Effect of collagen and mineral content on the high-frequency ultrasonic properties of human cancellous bone. Osteoporos Int 2002;13(1):26–32.
30. Riekkinen O, Hakulinen MA, Lammi MJ, Jurvelin JS, Kallioniemi A, Töyräs J. Acoustic properties of trabecular bone–relationships to tissue composition. Ultrasound Med Biol 2007;33(9):1438–44.
31. Langton CM, Njeh CF. The measurement of broadband ultrasonic attenuation in cancellous bone–a review of the science and technology. IEEE Trans Ultrason Ferroelectr Freq Control 2008;55(7):1546–54.
32. Kaleva E, Töyräs J, Jurvelin JS, Virén T, Saarakkala S. Effects of ultrasound frequency, temporal sampling frequency, and spatial sampling step on the quantitative ultrasound parameters of articular cartilage. IEEE Trans Ultrason Ferroelectr Freq Control 2009;56(7):1383–93.
33. Chérin E, Saïed A, Laugier P, Netter P, Berger G. Evaluation of acoustical parameter sensitivity to age-related and osteoarthritic changes in articular cartilage using 50-MHz ultrasound. Ultrasound Med Biol 1998;24(3):341–54.
34. Saarakkala S, Töyräs J, Hirvonen J, Laasanen MS, Lappalainen R, Jurvelin JS. Ultrasonic quantitation of superficial degradation of articular cartilage. Ultrasound Med Biol 2004;30(6):783–92.
35. Töyräs J, Laasanen MS, Saarakkala S, Lammi MJ, Rieppo J, Kurkijarvi J, *et al*. Speed of sound in normal and degenerated bovine articular cartilage. Ultrasound Med Biol 2003;29 (3):447–54.
36. Aula AS, Jurvelin JS, Töyräs J. Simultaneous computed tomography of articular cartilage and subchondral bone. Osteoarthritis Cartilage 2009;17(12):1583–8.
37. Töyräs J, Lyyra-Laitinen T, Niinimäki M, Lindgren R, Nieminen MT, Kiviranta I, *et al*. Estimation of the Young's modulus of articular cartilage using an arthroscopic indentation instrument and ultrasonic measurement of tissue thickness. J Biomech 2001;34(2):251–6.
38. Jurvelin JS, Räsänen T, Kolmonen P, Lyyra T. Comparison of optical, needle probe and ultrasonic techniques for the measurement of articular cartilage thickness. J Biomech 1995;28(2):231–5.
39. Hayes WC, Keer LM, Herrmann G, Mockros LF. A mathematical analysis for indentation tests of articular cartilage. J Biomech 1972;5(5):541–51.
40. Töyräs J, Rieppo J, Nieminen MT, Helminen HJ, Jurvelin JS. Characterization of enzymatically induced degradation of articular cartilage using high frequency ultrasound. Phys Med Biol 1999;44(11):2723–33.
41. Kiviranta I, Jurvelin J, Tammi M, Säämänen AM, Helminen HJ. Microspectrophotometric quantitation of glycosaminoglycans in articular cartilage sections stained with Safranin O. Histochemistry 1985;82(3):249–55.
42. Blumenkrantz N, Asboe-Hansen G. New method for quantitative determination of uronic acids. Anal Biochem 1973;54 (2):484–9.
43. Brown S, Worsfold M, Sharp C. Microplate assay for the measurement of hydroxyproline in acid-hydrolyzed tissue samples. Biotechniques 2001;30(1):38–40. 42.
44. Chérin E, Saïed A, Pellaumail B, Loeuille D, Laugier P, Gillet P, *et al*. Assessment of rat articular cartilage maturation using 50-MHz quantitative ultrasonography. Osteoarthritis Cartilage 2001;9(2):178–86.
45. Kaleva E, Saarakkala S, Jurvelin JS, Virén T, Töyräs J. Effects of ultrasound beam angle and surface roughness on the quantitative ultrasound parameters of articular cartilage. Ultrasound Med Biol 2009;35(8):1344–51.
46. Wilhjelm JE, Pedersen PC, Jacobsen SM. The influence of roughness, angle, range, and transducer type on the echo signal from planar interfaces. IEEE Trans Ultrason Ferroelectr Freq Control 2001;48(2):511–21.
47. Langton CM, Subhan M. Computer and experimental simulation of a cortical end-plate phase cancellation artefact in the measurement of BUA at the calcaneus. Physiol Meas 2001;22 (3):581–7.
48. Langton CM, Njeh CF, Hodgskinson R, Currey JD. Prediction of mechanical properties of the human calcaneus by broadband ultrasonic attenuation. Bone 1996;18(6):495–503.
49. Xia Y, Lin W, Qin YX. The influence of cortical end-plate on broadband ultrasound attenuation measurements at the human calcaneus using scanning confocal ultrasound. J Acoust Soc Am 2005;118(3 Pt 1):1801–7.
50. Karjalainen J, Riekkinen O, Töyräs J, Kröger H, Jurvelin J. Ultrasonic assessment of cortical bone thickness in vitro and in vivo. IEEE Trans Ultrason Ferroelectr Freq Control 2008;55 (10):2191–7.